Dynamic Characteristics of a DC Motor Controlled by Single-Phase Half-Wave Thyristor Rectifier Circuit (II)

By

Tsuguo ANDŌ* and Jūrō UMOTO*

(Received March 17, 1975)

Abstract

When the armature voltage of a dc motor is being controlled by a single-phase half-wave thyristor rectifier circuit, the armature current flows discontinuously, but the motor speed scarcely fluctuates during one cycle of an ac supply frequency. Hence, the authors analyse the static and dynamic characteristics of the dc motor for the case where it is assumed that the fluctuation of the motor speed is negligible. In the analysis, they consider the effects of the motor brush and thyristor internal voltage drops on the characteristics, which can't be neglected when the motor is driven with a low voltage supply. Next, they compare the theoretical results with the experimental ones; and then investigate the effects of circuit parameters on the characteristics of the motor. Finally, they make a study of the dissipated power, efficiency and frequency response in the circuit, which have not been investigated in the usual papers.

1. Introduction

The development of the control technique in recent years spreads the application of thyristor circuits in the speed control system of the motor. Therefore, it is necessary to research not only the static characteristics of the motor in the steady state, but also the dynamic ones, including the motor performances, in the transient state.

The authors study the characteristics of the dc motor controlled by thyristor rectifier circuits, which have excellent control ability, and are widely used nowadays. Already, they have derived a theoretical mothod to analyse the dynamic characteristics of the spearately excited dc motor controlled by the single-phase half-wave thyristor circuit[1], in which the fluctuation of the speed is considered during one cycle of the ac supply frequency.

On the other hand, with respect to the motor which usually has a large

* Department of Electrical Engineering.

moment of inertia, that fluctuation is almost suppressed. Consequently, we can analyse the motor characteristics with fair accuracy, even if we assume that the motor speed is constant during one cycle.

In this paper, the authors propose simplified methods to analyse the static and dynamic characteristics of the motor, which are applicable for the case where the fluctuation of the motor speed is very small. Next, they investigate theoretically and experimentally the effects of the circuit parameters in the motor control system on the characteristics of the motor.

2. Fundamental Equations

Fig. 1 shows the circuit diagram of a single-phase half-wave thyristor rectifier circuit, in which the speed n of the separately excited dc motor is controlled by changing the firing angle of the thyristor Th. In the figure, the current i begins to flow at the instant when Th is fired, and then driving torque $K_t i$ is supplied to the motor, where K_t is a torque coefficient of the motor. On the other hand, the stalled motor begins to rotate when $K_t i$ exceeds the static torque Q_s of the motor with a load. When i decreases to zero, i is interrupted by a reverse blocking characteristic of Th, and then the motor rotates by its inertia. But when the average value of $K_t i$ becomes smaller than the coulomb torque Q, the motor can't keep rotating and finally stops.

As described in the previous paper[1], the above circuit performances are divided into four fundamental modes, shown in Fig. 2, and can be analysed by the following equations

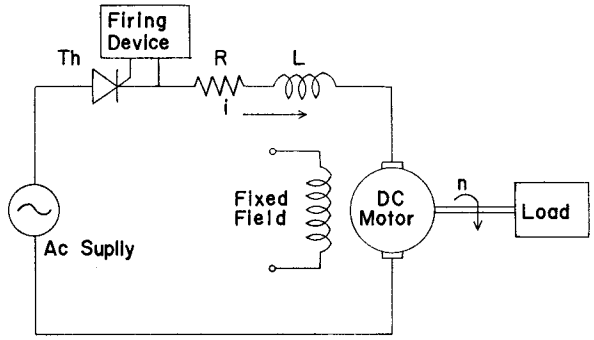

Fig. 1. Control circuit of separately excited dc motor.

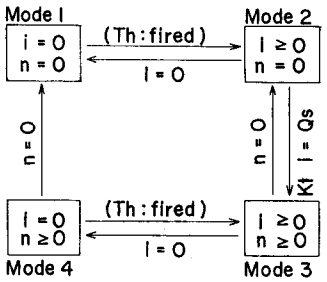

Fig. 2. Fundamental modes.

$$E_m \sin(\omega_0 t+\alpha) = L di/dt + Ri + K_v n + E_b, \tag{1}$$

$$K_t i = J dn/dt + Fn + Q, \tag{2}$$

where

E_m : maximum value of ac supply voltage,
E_b : brush voltage drop including thyristor voltage drop,
L : total inductance in armature circuit,
R : total resistance in armature circuit,
K_v : counter emf coefficient of motor,
J : moment of inertia of motor contained load,
F : viscous friction coefficient of motor with load,
t : time,
ω_0 : angular frequency of ac supply,
α : firing angle of thyristor Th.

Here, we assume that the motor armature reaction and the nonlinearlity of the circuit parameters can be neglected. Then, the above fundamental equations can be transformed to the following electrical equations

$$E_m \sin(\omega_0 t+\alpha) = Ldi/dt+Ri+v+E_b, \tag{3}$$

$$i = Cdv/dt+Gv+I_q, \tag{4}$$

where

$v=K_v n$: counter emf of motor,
$C=J/K_t K_v$: equivalent capacitance of J,
$G=F/K_t K_v$: equivalent conductance of F,
$I_q=Q/K_t$: equivalent forced current of Q.

The circuit performance in Fig. 1 can be analysed by using Fig. 2 and Eqs. (3) and (4). However, about the usual motor, the speed fluctuation during one cycle is almost suppressed by the moment of inertia. Therefore, we shall approximately analyse that performance under the assumption that the fluctuation can be neglected.

3. Static Characteristics

The counter emf v in Eq. (3) can be expressed by the constant voltage V under our assumption, and then we can obtain

$$E_m \sin(\omega_0 t+\alpha) = Ldi/dt+Ri+V+E_b. \tag{5}$$

Solving Eq. (5) under the condition that the initial value of i is zero, we get

$$i=[E_m\{\sin(\omega_0 t+\alpha-\delta)-\varepsilon^{-t/T_e}\sin(\alpha-\delta)\}\cos\delta - (V+E_b)(1-\varepsilon^{-t/T_e})]/R, \tag{6}$$

where

$T_e=L/R$: electrical time constant in armature circuit,

$\delta=\tan^{-1}(\omega_0 T_e)$.

Here, putting $i=0$ at $t=t_1$, we can obtain the following relation among V, t_1 and α

$$g(t_1)\equiv E_m\{\sin(\omega_0 t_1+\alpha-\delta)-\varepsilon^{-t_1/T_e}\sin(\alpha-\delta)\}\cos\delta - (V+E_b)(1-\varepsilon^{-t_1/T_e})=0, \tag{7}$$

where t_1 is the conductive duration of Th.

Next, integrating Eq. (3) from $t=0$ to t_1, the average value I_d of i is easily calculated as follows

$$I_d=\frac{1}{\tau}\int_0^{t_1} i\,dt = [E_m\{\cos\alpha-\cos(\omega_0 t_1+\alpha)\}-\omega_0 t_1(V+E_b)]/2\pi R, \tag{8}$$

where

$\tau=2\pi/\omega_0$: period of ac supply frequency.

Furthermore, by multiplying both sides of Eq. (3) by i and then integrating that result, we get

$$P_i=RI_e^2+P_0+E_bI_d, \tag{9}$$

where

$P_i=\frac{1}{\tau}\int_0^{t_1} iE_m\sin(\omega_0 t+\alpha)\,dt$: input power,

$P_0=\frac{1}{\tau}\int_0^{t_1} iV\,dt=VI_d$: output power,

$I_e=\left(\frac{1}{\tau}\int_0^{t_1} i^2dt\right)^{1/2}$: effective value of i.

Therefore, the motor efficiency η is given by

$$\eta=P_0/P_i, \tag{10}$$

where the mechanical no-load loss of the motor and the electrical power loss in in the field circuit are neglected.

Next, let us discuss the motor characteristic in the case where the values of the coefficients K_t, F and Q are given. The torque equation (2) is transformed to the electrical equivalent equation in the steady state, as follows

$$I_d=GV+I_q. \tag{11}$$

Then, from Eqs. (11) and (8), we have

$$V=\frac{E_m\{\cos\alpha-\cos(\omega_0 t_1+\alpha)\}/2\pi-t_1E_b/\tau-RI_q}{RG+t_1/\tau}. \tag{12}$$

Using this equation, we can analyse the motor characteristics.

4. Dynamic Chracteristics

As shown in the previous section, the relations of v, i, t_1 and I_d vs. α are expressed by the transcendental relations. It is very difficult to solve them exactly in the transient state. Therefore, we study the motor response with a small change of α, and then derive the approximate linear equations to analyse the dynamic characteritics.

Here we show two analytical methods. In these methods we regard the motor performance in the original circuit as the one in the equivalent continuous system, or in the sampled data system.

4.1 Equivalent Continuous System

We assume that V, I_d and t_1 vary by the small values ΔV, ΔI_d and Δt_1, respectively, when α changes by $\Delta\alpha$. We can deduce the following equations from Eqs. (7) and (8)

$$\left.\begin{aligned} &\frac{\partial g(t_1)}{\partial \alpha}\Delta\alpha+\frac{\partial g(t_1)}{\partial t_1}\Delta t_1+\frac{\partial g(t_1)}{\partial V}\Delta V=0,\\ &\Delta I_d=\frac{\partial I_d}{\partial \alpha}\Delta\alpha+\frac{\partial I_d}{\alpha t_1}\Delta t_1+\frac{\partial I_d}{\partial V}\Delta V. \end{aligned}\right\} \tag{13}$$

Eliminating Δt_1 from Eqs. (13), we get

$$\Delta I_d=A\Delta\alpha+B\Delta V, \tag{14}$$

where

$$\begin{aligned} A&=\frac{\partial I_d}{\partial \alpha}-\frac{\partial I_d}{\partial t_1}\frac{\partial g(t_1)}{\partial \alpha}\Big/\frac{\partial g(t_1)}{\partial t_1},\\ &=E_m[\sin(\omega_0 t_1+\alpha)-\sin\alpha-\{\cos(\omega_0 t_1+\alpha-\delta)\\ &\quad-\varepsilon^{-t_1/T_e}\cos(\alpha-\delta)\}\sin\delta]/2\pi R,\\ B&=\frac{\partial I_d}{\partial V}-\frac{\partial I_d}{\partial t_1}\frac{\partial g(t_1)}{\partial V}\Big/\frac{\partial g(t_1)}{\partial t_1},\\ &=\omega_0\{T_e(1-\varepsilon^{-t_1/T_e})-t_1\}/2\pi R. \end{aligned}$$

On the other hand, using Eq. (4), we can write ΔI_d by the following equation, namely

$$\Delta I_d=Cd\Delta V/dt+G\Delta V. \tag{15}$$

By eliminating ΔI_d from Eqs. (14) and (15), we can derive the first order transfer function $G(s)$ of the motor in Fig. 1, as follows

$$G(s)=\frac{\Delta V(s)}{\Delta\alpha(s)}=\frac{K_c}{sT_c+1}, \tag{16}$$

where

s : Laplace operator,
$\Delta V(s)$: s-function of ΔV,
$\Delta\alpha(s)$: s-function of $\Delta\alpha$,
$K_c=A/(G-B)$,
$T_c=C/(G-B)$.

Then, the dynamic performance of the circuit shown in Fig. 1 can be regarded as the one in the continuous system, of which the block diagram is shown in Fig. 3.

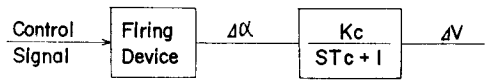

Fig. 3. Equivalent continuous system.

In connection with the derivation of the transfer function, the other two graphical methods were already presented in references 2) and 3). The results obtained by those methods gave a considerably good agreement with the experimental results. However, by using Eq. (16), the dynamic performance is analysed more directly.

4.2 Equivalent Sampled Data System

First we calculate i, t_1 and I_d, as described in section 3, under the assumption of $v=V$ (constant). Next, we solve the following equation

$$I_d=Cdv/dt+Gv+I_q, \tag{17}$$

derived from Eq. (4) under the assumption of $i=I_d$ (constant). Solving Eq. (17), we can obtain

$$v=(I_d-I_q)(1-\varepsilon^{-t/T_m})/G+V\varepsilon^{-t/T_m}, \tag{18}$$

where

$T_m=C/G$: mechanical time constant of motor with load.

From Eqs. (18) and (8) we obtain the variation ΔV of v during one period of the ac supply frequency, as follows:

$$\Delta V=(1-\varepsilon^{-\tau/T_m})[E_m\{\cos\alpha-\cos(\omega_0 t_1+\alpha)\}/2\pi -RI_q-t_1E_b/\tau-(RG+t_1/\tau)V]/RG. \tag{19}$$

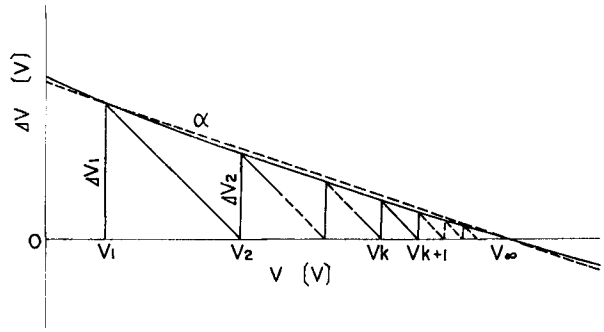

Fig. 4. Illustrative relation between V and ΔV.

Then, the relation between V and ΔV for the given firing angle α is illustrated by the curve as shown in Fig. 4.

As mentioned in reference 1), approximating the curve by the dotted straight line, the transient response of the motor is explained as follows. When the initial value and the variation of v in the first cycle are given by V_1 and ΔV_1, respectively, the value V_{k+1} of v after $k\tau$ seconds is expressed by:

$$\begin{aligned} V_{k+1} &= (1-m)V_k + mV_1 + \Delta V_1, \\ &= V_\infty \{1-(1-m)^k\} + V_1(1-m)^k, \end{aligned} \tag{20}$$

where

V_k: initial value of v during the k-th cycle,
$k = 1, 2, 3, \cdots\cdots$,
$m = -d\Delta V/dV$,
$V = \lim_{k\to\infty} V_k = V_1 + \Delta V_1/m$.

Here, V_∞ can be obtained by putting $\Delta V = 0$, and is equal to V given in Eq. (12). Also, m is calculated by Eqs. (19) and (7), as follows:

$$\begin{aligned} m &= -\left(\frac{\partial \Delta V}{\partial t_1}\frac{dt_1}{dV} + \frac{\partial \Delta V}{\partial V}\right), \\ &= (1-\varepsilon^{-\tau/T_m})\{RG + t_1/\tau - (1-\varepsilon^{-t_1/T_e})T_e/\tau\}/RG. \end{aligned} \tag{21}$$

In this connection, our approximate analysis can be applied to the case where $0<m<1$, because the fluctuation of v becomes large unless $0<m<1$.

Next, replacing the term $(1-m)$ in Eq. (20) by $\exp(-\tau/T_s)$, V_{k+1} is rewritten as:

$$V_{k+1} = V_\infty(1-\varepsilon^{-k\tau/T_s}) + V_1\varepsilon^{-k\tau/T_s}, \tag{22}$$

where T_s is an equivalent time constant of the motor, which is given by:

$$T_s = -\tau/\ln(1-m). \tag{23}$$

Consequently, we can see that the transient response of the motor in Fig. 1 is equivalent to the one in the first order sampled data system with a holding circuit, where the sampling period is τ seconds.

Now, let us consider the dynamic performance of the motor when α is changed by $\Delta\alpha$. In this case, the changes of the values of m and T_s are assumed to be very small and can be neglected. Then, we can set up the block diagram of the sampled data system as shown in Fig. 5, where the performance is equivalent to the one in Fig. 1. In Fig. 5, the gain parameter K_s is given by $dV_\infty/d\alpha$, and so K_s is equal to K_c in Eq. (16), namely

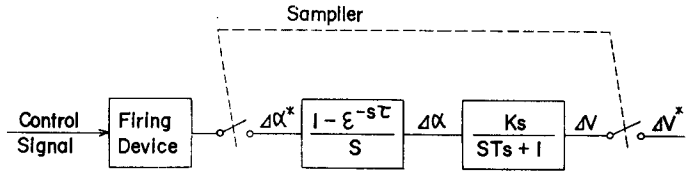

Fig. 5. Equivalent sampled data system.

$$K_s = dV_\infty/d\alpha = K_c. \tag{24}$$

The pulse transfer function $G^*(z)$ of the system in Fig. 5 is given by:

$$G^*(z) = \frac{\Delta V^*(z)}{\Delta\alpha^*(z)} = \frac{K_s z^{-1}(1-a)}{1-az^{-1}}, \tag{25}$$

where

$\Delta V^*(z)$: z-function of ΔV,
$\Delta\alpha^*(z)$: z-function of $\Delta\alpha$,
$z = \exp(s\tau)$,
$\alpha = \exp(-\tau/T_s)$.

The transfer function is useful when we wish to calculate the transient or frequency response of the motor. The transient response can be obtained by reversing the z-function $\Delta V^*(z)$ to the time function. On the other hand, when $\Delta\alpha$ is varied sinusoidally with the angular frequency ω, the frequency response is derived as follows:

$$G^*(z) = R_e + jI_m, \tag{26}$$

$z = \exp(j\omega\tau)$,
$j = \sqrt{-1}$,
$R_e = \dfrac{K_s(1-a)(\cos\omega\tau - a)}{1-2a\cos\omega\tau + a^2}$: real part of $G^*(z)$,
$I_m = \dfrac{K_s(1-a)\sin\omega\tau}{1-2a\cos\omega\tau + a^2}$: imaginary part of $G^*(z)$.

Then, the vector trajectory of $G^*(z)$ is plotted by the following circular equation

$$\left(R_e-\frac{aK_s}{1+a}\right)^2+I_m{}^2=\left(\frac{K_s}{1+a}\right)^2. \tag{27}$$

5. Numerical Calculations and Experimental Results

In the above sections, we have derived the simplified analysis of the static and dynamic characteristics of the motor control circuit in Fig. 1. So, in this section, in order to investigate the appropriateness of our analysis, we make an experiment with the small sized dc servo-motor, where the specification of the motor and the circuit parameters are shown in Tables 1 and 2. Then, we compare the experimental results with the numerical calculation results.

Table 1. Specification of the dc servo-motor.

Type (Maker)	JKMM-6EM (Yasukawa Electric Co.)
Rated Power	190 〔W〕
Rated Voltage	40 〔V〕
Rated Current	6 〔A〕
Rated Speed	3000 〔rpm〕
Field Excitation	Permanent Magnet

Table 2. Circuit parameters.

Mechanical Parameters		Electrical Parameters	
J =0.011	〔kg•m〕	C=0.0313	〔F〕
Q =0.420 to 0.203	〔N•m〕	I_q=0.710 to 0.342	〔A〕
F =0.00499 to 0.174	〔N•m•s/rad〕	G=28.5 to 497.4	〔m℧〕
		E_m=70.7	〔V〕
Q_s =0.503	〔N•m〕	E_b =3.02	〔V〕
K_v=0.592	〔V•s/red〕	R=6.03	〔Ω〕
K_t=0.592	〔N•m/A〕	L =0.9, 20.9, 40.9	〔mH〕
		ω_0 =377	〔rad/s〕

5.1 Static Characteristics

Fig. 6 shows the calculated relations between I_d and V for several values of L and α, which correspond to the speed-torque characteristics of the motor. Next, Figs. 7(a) and (b) illustrate the calculated relations of $V, I_e, P_i, t_1/\tau$ and η vs. I_d for $\alpha=2\pi/9$ 〔rad〕, L=0.9 〔mH〕 and L=40.9 〔mH〕. Fig. 8 presents the relations of $V, I_d, I_e, P_i, t_1/\tau$ and η vs. α for G=56.5, 〔m℧〕, I_q=0.672 〔A〕 and

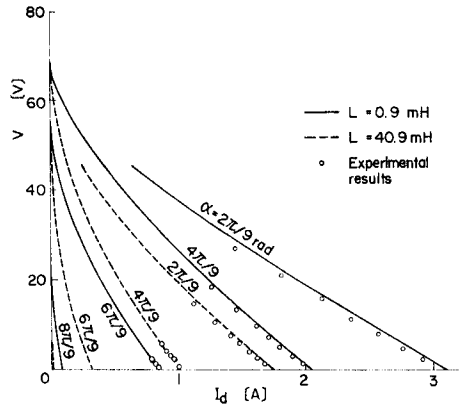

Fig. 6. Relation between I_d and V for $L=0.9$ and 40.9 [mH].

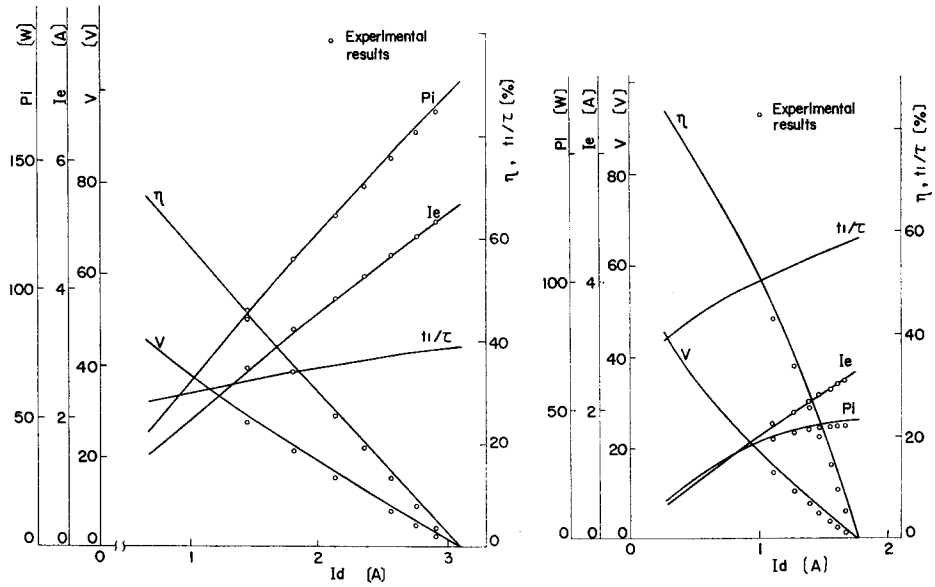

(a) $L=0.9$ [mH]. (b) $L=40.9$ [mH].

Fig. 7. Static characterictics for $\alpha=2\pi/9$ [rad].

$L=0.9$ [mH]. In these figures, some experimental results are also marked. Here, we must notice that the thyristor can't be fired for $E_m \sin\alpha < V$ and the motor rests for $I_d < I_q$.

Fig. 9 shows the calculated and experimental examples of the waveforms of i and v for $\alpha=2\pi/9$ [rad].

From the figures, we can confirm the validity of our assumption, that the fluctuation of v can be neglible. Furthermore, we can see that the conducting

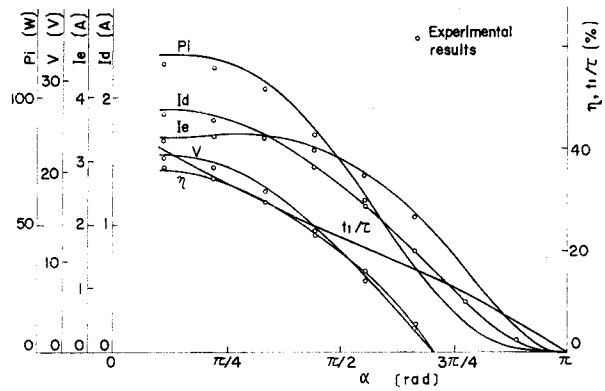

Fig. 8. Relations of V, I_d, I_e, P_i, t_1/τ and η vs. α for $G=56.5$ [m℧], $I_q=0.672$ [A] and $L=0.9$ [mH].

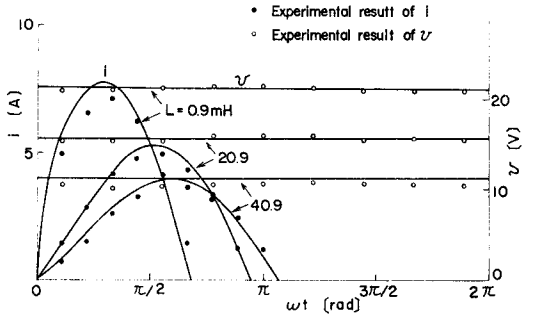

Fig. 9. Waveforms of i and v for $G=56.5$ [m℧], $I_q=0.672$ [A] and $\alpha=2\pi/9$ [rad].

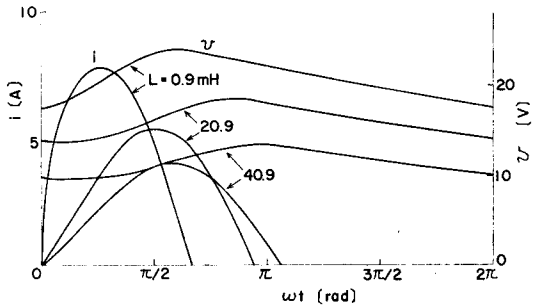

Fig. 10. Waveforms corresponding to Fig. 9 when $C=0.00313$ [F].

duration of i increases, but the values of i and v decrease when we increase the value of L.

However, our analytical method can't be used when the value of C, corresponding to the moment of the motor inertia, is small and the fluctuation of v

is recognized as shown in Fig. 10. In the figure, the value of C is decreased to ten per cent of the value in Fig. 9, and the waveforms are calculated by the exact method derived previously[1].

5.2 Dynamic Characteristics

In Figs. 11 and 12, we plot the calculated relations of K_s and T_s vs. α, which are obtained with Eqs. (24) and (23), respectively. Since K_s and T_s are fairly influenced by α, we can use the block diagram shown in Fig. 5 only in a limited range, where $\Delta\alpha$ is very small for the basic firing angle α.

In this connection, the α-T_c curves obtained by Eqs. (16) correspond to the α-T_s curves in Fig. 12 very well.

In Fig. 13, we plot the transient values of V_k, which are calculated by Eq. (22) for the following conditions:

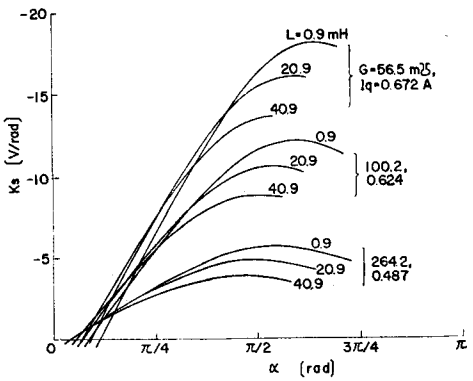

Fig. 11. Relation between K_s and α.

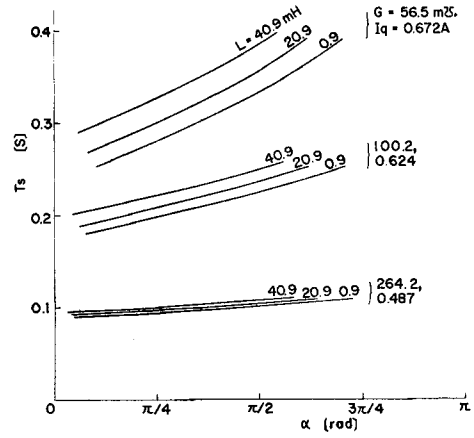

Fig. 12. Relation between T_s and α.

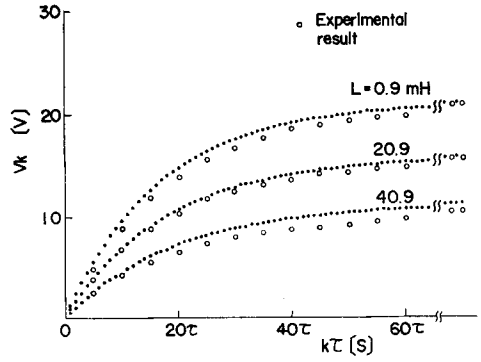

Fig. 13. Transient response of V for $\alpha=2\pi/9$ [rad].

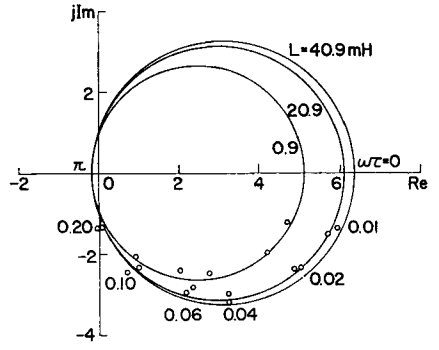

Fig. 14. Frequency response of $-\Delta V$ for $\alpha=2\pi/9$ [rad].

G =56.5 〔m℧〕, I_q=0.672 〔A〕,
V_1=0 〔V〕, α =2π/9 〔rad〕,
L =0.9, 20.9 and 40.9 〔mH〕,
T_s=0.276, 0.296 and 0.323 〔s〕,
V_∞=21.0, 15.7 and 11.1 〔V〕.

Also in this figure, we show the experimental results, which agree well with the calculated results.

In Fig. 14, we represent the frequency responses of the motor, which are calculated by Eqs. (26) and (27) for

G =56.5 〔m℧〕, I_q=0.672 〔A〕,
α =2π/9 〔rad〕: basic firing angle,
L =0.9, 20.9 and 40.9 〔mH〕,
K_s=−5.08, −6.08 and −6.30 〔V/rad〕,

and also add some experimental results for $\Delta\alpha=0.38\sin\omega t$.

Next, let us consder the response of the motor in the case where we use the block diagram of the equivalent continuous system described in section 4.1. Since the following relations

$$K_c=K_s,\quad T_c\fallingdotseq T_s,\quad T_c>\tau,$$

are satisfied, the transient response becomes identical to the one of the equivalent sampled data system shown in Fig. 5. On the other hand, with respect to the frequency response, we can't obtain the sampling characteristic of the original circuit. Hence, we must use the block diagram as shown in Fig. 5, in order to analyse the dynamic characteristic of the motor accurately.

6. Conclusions

In this paper, the authors have introduced an approximate method to analyse the static and dynamic characteristics of the dc motor controlled by the single-phase half-wave thyristor rectifier circuit. Also, they have verified the validity of their method by comparing the calculated results with the experimental ones about both characteristics. Furthermore, they have investigated the influence of the circuit parameters on the motor performance.

Now, this simplified method is applicable to analyse the characteristics of the motor controlled by other types of thyristor circuits, where the armature current is interrupted periodically, and the fluctuation of the motor speed is almost suppressed. In particular, the block diagram shown in Fig. 5 will be applicable to analyse the motor performance when the speed feedback is adopted to the original circuit.

Acknowledgements

The authors wish to thank Messrs. C. Kobayashi and R. Mantani for their halp in the experiment and the numerical calculations.

References

1) T. Ando and J. Umoto; THIS MEMOIRS, **34**, 103 (1972).
2) O. Ishizaki and S. Ishikawa; J. Inst. Elect. Engrs. Japan, **83**, 1201 (1963).
3) K. Nitta, Y. Okitsu, T. Suzuki and Y. Kinouchi; ibid., **90**, 1577 (1970).